

Particle-in-cell simulation for the effect of magnetic cusp on discharge characteristics in a cylindrical Hall thruster

Sheng-Tao Liang(梁圣涛), Hui Liu(刘辉), Da-Ren Yu(于达仁)
Citation: Chin. Phys. B . 2018, 27(4): 045201. **doi:** 10.1088/1674-1056/27/4/045201

Journal homepage: http://cpb.iphy.ac.cn; http://iopscience.iop.org/cpb

What follows is a list of articles you may be interested in

Particle-in-cell simulation for different magnetic mirror effects on the plasma distribution in a cusped field thruster

Liu Hui, Chen Peng-Bo, Zhao Yin-Jian, Yu Da-Ren
Chin. Phys. B . 2015, 24(8): 085202. **doi:** 10.1088/1674-1056/24/8/085202

Three-dimensional PIC/MCC simulation of electron deposition in JAEA 10 A ion sources

Yang Chao, Yin Mao-Wei, Shang Li-Ping, Wei Ai-Yong
Chin. Phys. B . 2014, 23(9): 095201. **doi:** 10.1088/1674-1056/23/9/095201

Numerical study on the electron-wall interaction in a Hall thruster with segmented electrodes placed at the channel exit

Qing Shao-Wei, E Peng, Duan Ping, Xu Dian-Guo
Chin. Phys. B . 2013, 22(8): 085203. **doi:** 10.1088/1674-1056/22/8/085203

Using short pulses to enhance the production rate of vibrationally excited hydrogen molecules in hydrogen discharge

Sun Ji-Zhong,Li Xian-Tao,Bai Jing,Wang De-Zhen
Chin. Phys. B . 2012, 21(5): 055205. **doi:** 10.1088/1674-1056/21/5/055205

Particle-in-cell simulation for the effect of magnetic cusp on discharge characteristics in a cylindrical Hall thruster*

Sheng-Tao Liang(梁圣涛), Hui Liu(刘辉)†, and Da-Ren Yu(于达仁)

Laboratory of Plasma Propulsion, Harbin Institute of Technology, Harbin 150001, *China*

(Received 16 November 2017; revised manuscript received 2 January 2018; published online 29 March 2018)

The cylindrical Hall thruster has the good prospect of serving as a miniaturized electric propulsion device. A 2D-3V particle-in-cell plus Monte Carlo (PIC-MCC) method is used to study the effect of the magnetic cusp on discharge characteristics of a cylindrical Hall thruster. The simulation results show that the main ionization region and the main potential drop of the thruster are located at the upstream of the discharge channel. When the magnetic cusp moves toward the anode side, the main ionization region is compressed and weakened, moving upstream correspondingly. The ionization near the cusp is enhanced, and the interaction between the plasma and the wall increases. The simulation results suggest that the magnetic cusp should be located near the channel exit.

Keywords: cylindrical Hall thruster, PIC-MCC method, magnetic cusp

PACS: 52.65.Pp, 52.65.Rr, 52.75.Di **DOI:** 10.1088/1674-1056/27/4/045201

1. Introduction

Low power electric propulsion has become a competitive technology for small satellite propulsion system due to its advantages of high specific impulse and extended life.[1] Hall thrusters have been widely used in spacecraft and developed to achieve a relatively high performance at a power above 0.5 kW.[2] However, scaling down the hall thrusters to low power space applications has several challenges due to its large surface-to-volume ratio and difficulty in miniaturizing the magnetic circuit, which would aggravate the channel wall erosion and limit the thruster lifetime.[3] The cylindrical Hall thruster (CHT) raised by Raitses seems to be more promising as a miniaturized electric propulsion device.[4]

The magnetic field of the CHT is similar to that of the end-Hall ion source.[5] The divergent magnetic field has a large axial component, especially in the center of the channel. The radial magnetic field component increases near the channel wall. The magnetic field has a clear negative gradient property and maximizes at the entrance of discharge channel. The working mechanism of the CHT differs from that of the conventional Hall thruster. In the unique magnetic field configuration of the CHT, the confinement type of electrons is very different from the azimuthal $\boldsymbol{E}\times\boldsymbol{B}$ drift in conventional Hall thruster. In the CHT, electrons are trapped axially in a hybrid magnetoelectrostatic trap which is formed by the magnetic mirror near the anode side and the electric field near the channel exit side. The electrons can move back and forth axially in the discharge channel to enhance ionization. The CHT has a reduced surface-to-volume ratio, limiting ion losses and electron transport.[6] The CHT has been investigated as a means of improving the performances of miniaturized Hall thrusters.

The magnetic field of the CHT can be generated by either electromagnet coils or permanent magnets. Comprehensive studies of the CHT with electromagnetic coils have already been reported. It was found that for the miniaturized 100 W–200 W-class CHTs, the optimal magnetic field configuration is of a magnetic mirror-type. The thruster can achieve the highest performance parameters when the maximum magnetic field at the mirror was 1.5 kGs–2 kGs,[7] (1 Gs = 10^{-4} T). In this regime, the electromagnetic coils consumed 50 W–100 W. For the low power thruster, this additional power consumption reduces the overall thruster efficiency drastically. The using of permanent magnets instead of electromagnet coils can offer a significant reduction of both the total electric power consumption and the mass. Due to the engineering demand for a CHT with good radiating capability and high reliability, it is necessary to use permanent magnets with a circular structure, which can be conducive to heat dissipation and prevent the anode from overheating,[8] but easy to form the magnetic cusp in the channel.[9] It is necessary to explore the influence of the cusp characteristics on the discharge process of the CHT.

Most experimental studies on the CHT are based on the probe diagnostics in the plume,[10] which is difficult to obtain the plasma parameters inside the discharge channel. Numerical simulation is regarded as a particularly effective tool to obtain the characteristics of plasma parameter distributions.[11–13] The numerical simulation of the CHT with different magnetic cusp characteristics is analyzed in this paper by the particle-in-cell plus Monte Carlo (PIC-MCC) method. The rest of this paper is organized as follows. In

*Project supported by the National Natural Science Foundation of China (Grant Nos. 11505041 and 51776047).

†Corresponding author. E-mail: huiliu@hit.edu.cn

© 2018 Chinese Physical Society and IOP Publishing Ltd

Section 2, the thruster structure and magnetic circuit are introduced. In Section 3, the PIC-MCC simulation model is introduced. In Section 4, the results of the numerical simulation are presented and analyzed. Finally, several conclusions are drawn in Section 5.

2. Thruster structure and magnetic circuit

In this paper, the thruster utilizes a permanent magnetic ring to produce magnetic field. Figure 1 shows the cross-sectional view of the CHT. The thruster has a cylindrical discharge channel, with the anode located at the upstream end of the discharge channel. The radius and length of the discharge channel are 10 mm and 15 mm, respectively. The location of the magnetic cusp is adjusted by changing the length of the front magnetic pole, i.e., case 1 (L = 13 mm), case 2 (L = 9 mm), and case 3 (L = 5 mm). The magnetic field distributions along the axial direction and the channel wall direction are shown in Figs. 2(a) and 2(b), respectively. It can be found

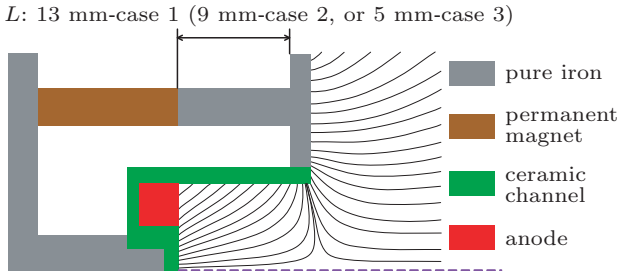


Fig. 1. (color online) Schematic diagram of thruster structure and magnetic field configuration.

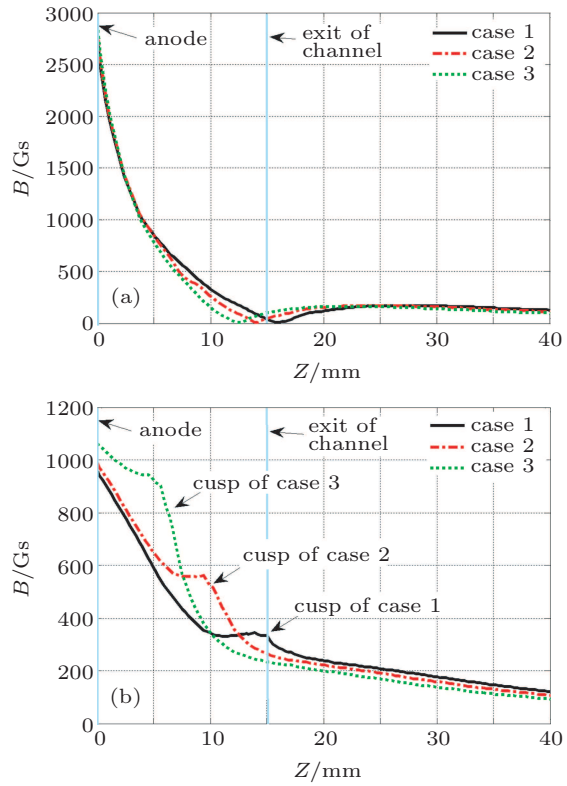


Fig. 2. (color online) Magnetic field distributions in (a) axial direction and (b) channel wall direction under different magnetic cusp characteristics.

from the figure that the magnetic field strengths on the axis are approximately the same, but the magnetic field strengths near the cusp increase when the cusp moves toward the anode side.

3. Simulation models

In the 2D-3V axially symmetrical PIC-MCC model employed is the particle-in-cell method combined with Monte-Carlo techniques to simulate the positions, velocities, and energies of the neutral gas, electrons, and ions. This model we developed has been used to study the near-wall conductivity,[14] magnetic mirror effect,[15] and double-stage Hall thruster.[16] The magnetic field is imported from the results calculated by the FEMM software.

Figure 3 illustrates the simulation domain of the CHT adopted in this study. The simulation domain contains a discharge channel with a length of 15 mm and radius of 10 mm. A plume region with a length of 15 mm and radius of 20 mm is also considered in the model. The boundaries in counterclockwise direction are the dielectric, anode, dielectric, magnetic pole, free side, cathode, free side, and symmetry boundary, respectively.

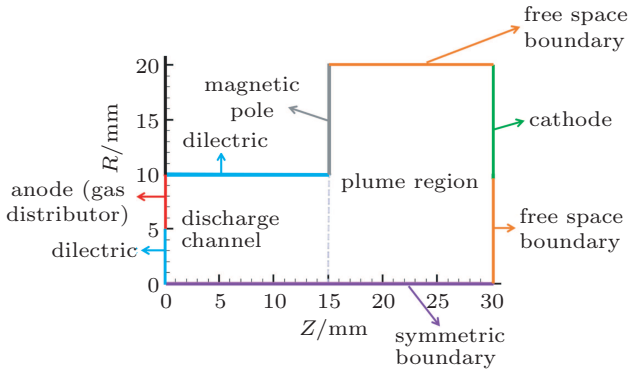


Fig. 3. (color online) Simulation domain of the cylindrical Hall thruster.

The anode mass flow rate is 0.2 mg/s and the voltage applied to the anode is 250 V. The cathode boundary is at the ground potential, and a quasi-neutrality cathode model is used to inject electrons into the computational domain at a temperature T_e = 5 eV. The magnetic pole boundary has a floating potential determined by the net charge collected and a capacitance with a fixed value. When particles hit the metallic boundary (the anode and the magnetic pole), electrons and ions are eliminated. Any particle moving across the free space boundaries would be eliminated. Any particle which crosses the symmetry boundary is specularly reflected.

The electron and ion densities are obtained via the simulation of their trajectories. The Boris's leapfrog method is used to study the particle movement. The initial speed of new particles is determined according to the half-Maxwell distribution, and the Poisson equation is solved using the dynamic alternating direct implicit method. The elastic scattering, excita-

tion and single ionization between electron and neutral atoms are modeled by the MCC technique, while the ion-neutral, Coulomb collisions and three-body and radiative recombinations are neglected because of their small collision frequency. At the end of each electron loop, ions are created at the ionization locations. The initial ion velocity is set to be equal to the local neutral background velocity.

Secondary electron emission (SEE) is considered at the dielectric walls. The SEE and electric field models we used at dielectric walls were proposed by Morozov.[17] The electric field at the dielectric surface is $E_\perp = \sigma/\varepsilon_0$, where $E_\perp$ is the electric field perpendicular to the wall, and σ is the surface charge density collected by the wall. The ε_0 is the vacuum permittivity coefficient. To reduce the computation time, the ε_0 is increased by a factor of γ^2 to reduce the numbers of grids and iterations. However, the larger artificial permittivity can also lead to more serious charge unbalance. By testing the different values of γ^2, it is found that the charge unbalance degree changes little when $\gamma^2 < 1600$. So we set γ^2 to be 1600. The feasibility of this method has already been proved in our simulation work before.[18]

The time step Δt equals the smaller value of $0.35/\omega_c$ and $0.1/\omega_{pe}$, where ω_c is the electron cyclotron frequency and ω_{pe} is the plasma oscillation frequency. The cell size $\Delta R = \Delta Z = 0.5$ mm is chosen to ensure that it is smaller than the smallest Debye length in the thruster. This 2D-3V PIC-MCC model is used to study the discharge characteristics of the low-power CHT. After about two-day calculation, the result of steady state is obtained successfully.

4. Simulation results and discussion

Figure 4 shows the ion density distributions for different locations of the magnetic cusp. It can be found that the main ionization region is located in the middle region between the anode and the magnetic cusp. The ionization near the cusp is very weak. One reason is due to the low density of the atom at the cusp, since the cusp is located at the downstream of the channel. Another reason is that the main potential drop concentrates near the upstream anode (as shown in Fig. 6), resulting in electrons near the cusp unable to obtain sufficient energy ionizing the propellant.

The simulation results show a clear phenomenon of hollow plume, which accords well with PPPL experimental measurements of the permanent-magnet CHT.[19] It can be explained as follows. The magnetic field in the plume region has a large axial component, resulting in a large radial component of the electric field. Ions which are produced in the main ionization region and the region near the cusp cannot concentrate on the axis under the action of radial electric field.

Figure 5 shows the ion density distributions in the axial direction and the wall direction. The axial peak ion densities of the case 1, case 2, and case 3 are 2.34×10^{17} m^{-3}, 2.34×10^{17} m^{-3}, 2.04×10^{17} m^{-3}, respectively. The wall peak ion densities of the case 1, case 2, and case 3 are 5.28×10^{16} m^{-3}, 8.81×10^{16} m^{-3}, 9.28×10^{16} m^{-3}, respectively. As the magnetic cusp moves toward the anode side, the ion density decreases in the main ionization region but increases near the magnetic cusp. The main ionization region is compressed and the main ionization process decreases. The ionization enhancement near the magnetic cusp is due to the increased magnetic field strength at the cusp, which enhances the electron confinement there.

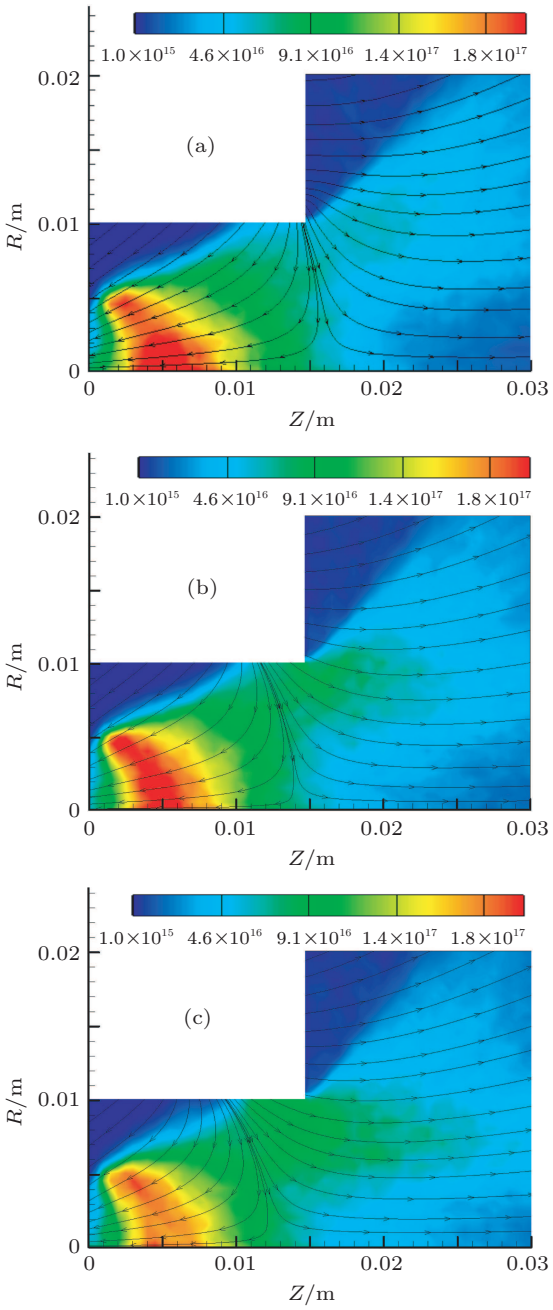


Fig. 4. (color online) Ion density distributions for (a) case 1, (b) case 2, (c) case 3.

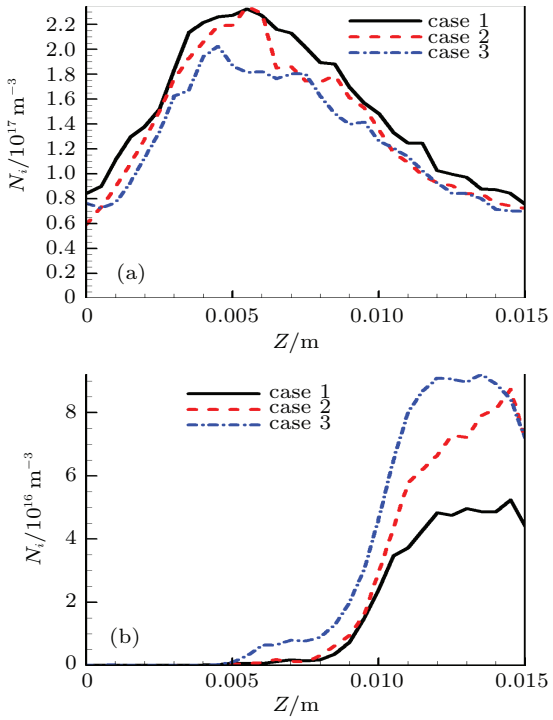


Fig. 5. (color online) One-dimensional (1D) axial ion density distributions on (a) channel axis and (b) the channel wall.

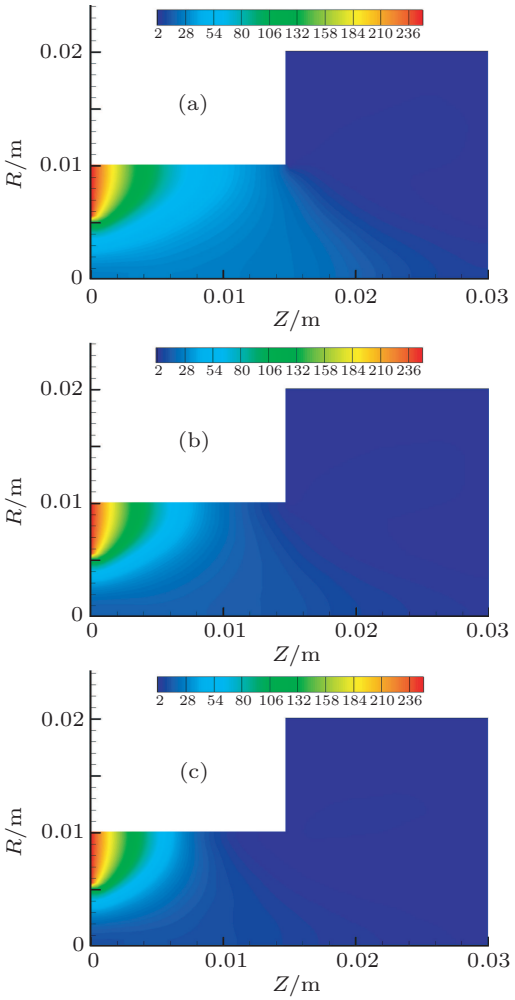


Fig. 6. (color online) Potential distributions for (a) case 1, (b) case 2, and (c) case 3.

Figure 6 displays the potential distributions. The simulation results show that the potential drops continuously from the anode to the exit of the channel, with the main potential drop focusing near the anode side. The reason is that the magnetic field strength of the magnetic mirror on the anode side is about 2700 Gs (1 Gs = 10^{-4} T), which is stronger and can better confine electrons than the magnetic field near the cusp where the value is about 350 Gs–800 Gs. So the main potential drop concentrates on the anode side, which accords well with previous experimental measurements.[20]

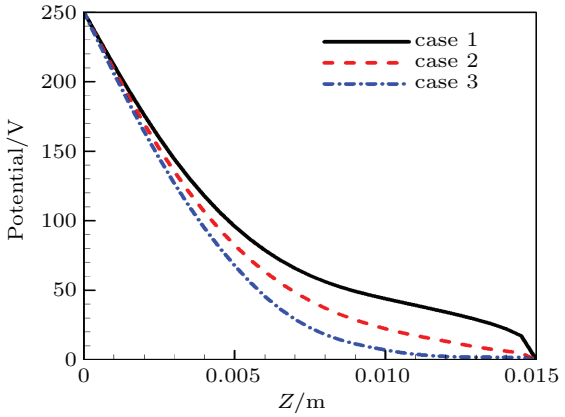


Fig. 7. (color online) 1D axial potential distributions on the channel wall.

Figure 7 presents the axial potential distributions on the wall of the ceramic channel. The distances between the anode (250 V) and the wall position whose potential is 50 V are 8.6 mm, 6.9 mm, and 5.8 mm for case 1, case 2, and case 3, respectively. When the magnetic cusp moves toward the anode side, the magnetic field of the cusp increases (see Fig. 2), leading to the increase of the electron confinement. Thus, the upstream electron mobility decreases and the main potential drop in the channel is clearly pushed to the anode side, which is not conducive to ion acceleration.

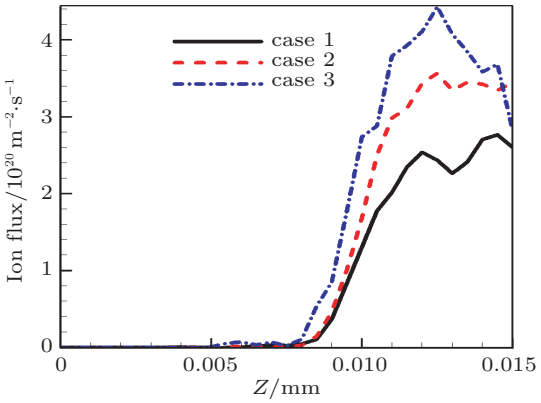


Fig. 8. (color online) 1D axial ion flux distributions on the channel wall.

Figure 8 shows the ion flux distributions on the wall. The peak fluxes for cases 1–3 are 2.78×10^{20} m^{-2}·s^{-1}, 3.57×10^{20} m^{-2}·s^{-1}, and 4.40×10^{20} m^{-2}·s^{-1}, respectively. As the

magnetic cusp moves toward the anode side, the ion accumulation increases near the magnetic cusp. Thus, the ion flux increases, resulting in more serious ion bombardment on the wall.

5. Conclusions

In this paper, the effect of the magnetic cusp on discharge characteristics of cylindrical hall thruster is studied by the PIC-MCC method. Special attention is paid to the plasma parameter distribution inside the discharge channel. The simulation results are as follows. The main ionization region and the main potential drop are located at the upstream of the channel. As the magnetic cusp moves toward the anode side, the main potential drop and the main ionization region move upstream correspondingly, and the main ionization process weakens. In this process, the ionization near the cusp is enhanced, increasing the interaction between the plasma and the wall. The simulation results suggest that the magnetic cusp should be located near the exit.

References

[1] Gorshkov O A 1998 34*th AIAA/ASME/SAE/ASEE Joint Propulsion Conference and Exhibit*, July 13–15, Cleveland, OH, USA, AIAA-1998-3929

[2] Miyasaka T, Uyama Y, Yoshida M, Miyake Y, Shimizu D, Goto R and Sakoda M 2017 *Vacuum* **136** 184

[3] Warner N Z 2007 "Theoretical and experimental investigation of Hall thruster miniaturization", Ph. D. dissertation (Massachusetts Institute of Technology)

[4] Smirnov A N, Raitses Y and Fisch N J 2002 *J. Appl. Phys.* **92** 5673

[5] Kaufman H R, Robinson R S and Seddon R I 1987 *J. Vac. Sci. Technol. A: Vacuum, Surfaces, Film* **5** 2081

[6] Smirnov A N, Raitses Y and Fisch N J 2003 *J. Appl. Phys.* **94** 852

[7] Smirnov A N, Raitses Y and Fisch N J 2004 *Phys. Plasmas* **11** 4922

[8] Kakuma T, Ikeda T, Nishida M, Kagota T, Takahata Y and Tahara H 2015 34*th International Electric Propulsion Conference and* 6*th Nano-satellite Symposium*, July 4–10, Hyogo-Kobe, Japan, IEPC-2015-302/ISTS-2015-b-302

[9] Polzin K A, Sooby E S, Kimberlin A C, Raitses Y, Merino E and Fisch N J 2009 45*th AIAA/ASME/SAE/ASEE Joint Propulsion Conference & Exhibit*, August 2–5, Denver, Colorado, USA, AIAA-2009-4812

[10] Gao Y Y, Liu H, Hu P, Huang H Y and Yu D R 2016 *Plasma Sources Sci. Technol.* **25** 35011

[11] Fu H and Scales W A 2013 *Phys. Plasmas* **20** 073704

[12] Xia G Q, Han Y J, Wu Q Y, Chen L W and Zhou N D 2017 *Plasma Chemistry and Plasma Processing* **37** 1505

[13] Xia G Q, Wu Q Y, Chen L W, Cong S Y and Han Y J 2017 *Contributions to Plasma Physics* **57** 377

[14] Yu D R, Li H, Wu Z W and Mao W 2007 *Phys. Plasmas* **14** 064505

[15] Liu H, Chen P B, Zhao Y J and Yu D R 2015 *Chin. Phys. B* **24** 085202

[16] Yu D R, Song M J, Liu H, Ding Y J and Li H 2012 *Phys. Plasmas* **19** 033503

[17] Morozov A I 1991 *J. Plasma Phys.* **17** 393

[18] Zhao Y J, Liu H, Yu D R and Wu H 2014 *J. Phys. D: Appl. Phys.* **47** 45201

[19] Raitses Y, Merino E and Fisch N J 2010 *J. Appl. Phys.* **108** 093307

[20] Smirnov A N, Raitses Y and Fisch N J 2007 *Phys. Plasmas* **14** 057106